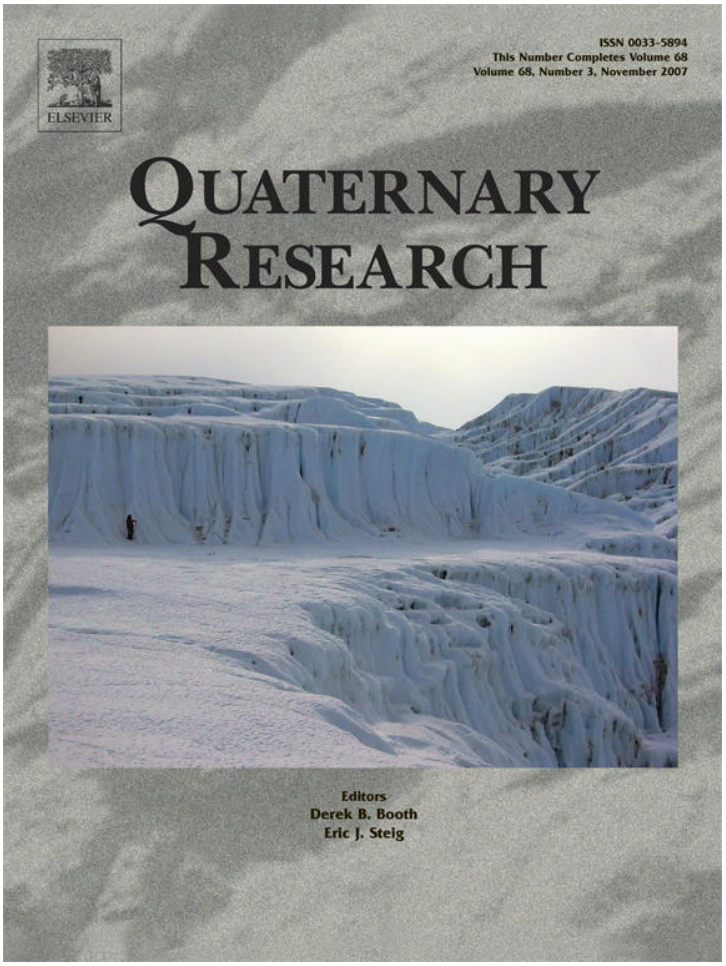

Available online at www.sciencedirect.com
ScienceDirect
Quaternary Research 68 (2007) 314–324
QUATERNARY RESEARCH
www.elsevier.com/locate/yqres

A new approach to detecting vegetation and land-use change using high-resolution lipid biomarker records in stalagmites

Alison J. Blyth [a,*], Asfawossen Asrat [b], Andy Baker [c], Pauline Gulliver [d], Melanie J. Leng [e,f], Dominique Genty [g]

[a] School of Civil Engineering and Geosciences, Drummond Building, University of Newcastle, Newcastle Upon Tyne, NE1 7RU, UK
[b] Department of Earth Sciences, Addis Ababa University, P.O. Box 1176, Addis Ababa, Ethiopia
[c] School of Geography, Earth and Environmental Sciences, The University of Birmingham, Edgbaston, Birmingham, B15 2TT, UK
[d] NERC Radiocarbon Laboratory, Scottish Enterprise Technology Park, Rankine Avenue, East Kilbride, Glasgow G75 0QF, UK
[e] NERC Isotope Geosciences Laboratory, British Geological Survey, Keyworth, Nottingham, NG12 5GG, UK
[f] School of Geography, University of Nottingham, Nottingham, NG7 2RD, UK
[g] LSCE, UMR CEA/CNRS 1572, L'Orme des Merisiers CEA Saclay, 91191 Gif/Yvette Cedex, France

Received 5 March 2007

Abstract

A hundred-year stalagmite lipid biomarker record from Mechara, southeastern Ethiopia, is presented. The record has been recovered at a 10-yr temporal resolution, marking the first time this has been achieved in stalagmite biomarker work and providing the first opportunity to investigate the relationship between stalagmite lipid records and hydrological transport lags, a vital issue in interpreting palaeoenvironmental signals. Preserved plant-derived *n*-alkanes and *n*-alkanols show clear changes in composition over time, relating to known land-use changes in the area, particularly the expansion of agriculture in the early twentieth century. The level of environmental detail provided by this technique, combined with the long-term chronological framework offered by stalagmites, holds significant promise for the investigation of early human environments and their associated climatic and anthropogenic controls.

Keywords: Stalagmite; Vegetation; Land use; Agriculture; *n*-Alkane; Lipid; Biomarker

Introduction

Understanding the relationship between past human populations and their natural environments is a major concern in archaeology and Quaternary science, being central to issues such as the spread of agriculture and the response of societies to climatic change. Fluctuations in past vegetation are generally investigated using microfossil analysis, particularly pollen cores (e.g., Dark, 2006, and references therein), which offer considerable detail about the composition of the dominant vegetation regime. However, these analyses are subject to limitations in the form of taphonomic disturbances and problems of preservation (Dimbleby, 1985; Horrocks and Lawlor, 2006). Here we present a new chemical approach to interpreting past vegetation change based upon the plant-derived biomolecules preserved in stalagmites.

Stalagmites have been widely used in studies of past environmental change (see Lauritzen and Lundberg 1999; McDermott, 2004, and references therein), in both the investigation of climatic changes and identifying fluctuations in vegetation regimes. They form as incremental mounds where drip-waters supersaturated with calcite enter caves. This mechanism of deposition provides an intimate link to the surrounding environment and climate, as the drip-water also carries chemical signals derived from the overlying soil. These include oxygen and carbon isotopes, trace elements and organic matter.

* Corresponding author. Present address: The McDonald Institute for Archaeological Research, University of Cambridge, Downing Street, Cambridge, CB2 3ER, UK. Fax: +44 1223 333536.
E-mail address: ajb259@cam.ac.uk (A.J. Blyth).

0033-5894/$ - see front matter © 2007 University of Washington. All rights reserved.
doi:10.1016/j.yqres.2007.08.002

Among this transported material are lipid biomarkers: these are biologically derived compounds that are indicative of different organism groups and so can be used to identify and trace inputs of different organic sources to an environmental record (Brassell et al., 1986; Meyers, 1997). They are increasingly widely used in sediment-based research for this purpose and to investigate climatic impacts on different environmental systems (e.g., Huang et al., 1999; Nott et al., 2000). A number of studies have also investigated the relationship between lipid compositions and different terrestrial ecosystems, demonstrating that certain compound distributions can relate to specific dominant vegetation regimes (Marseille et al., 1999; Bull et al., 2000; Pancost et al., 2002).

The biomarker data reported here center on high-molecular-weight (HMW) *n*-alkanes: straight-chain hydrocarbons with a chain length of twenty-five or more carbon atoms. These are frequently derived from higher plant waxes, a source indicated by an *n*-alkane distribution with a strong odd-over-even carbon number predominance (Bray and Evans, 1961; Eglinton and Hamilton, 1967). Research has shown that different carbon chain lengths are dominant in different plant types, providing potential for identifying vegetation change from the molecular signature preserved (Marseille et al., 1999; Rieley et al., 1991; Pancost et al., 2002). Additional results are presented from the HMW *n*-alkanols and HMW *n*-fatty acids, which also relate to the type of vegetation present and the amount of plant-derived input to the soil (Bull et al., 2000; Wiesenberg et al., 2004).

Analysing the lipid biomarker records preserved in stalagmites has great potential for both climatic and archaeological research. Stalagmites have an advantage over many other archives of the terrestrial environment in that they can be routinely chemically dated back to at least 500,000 yr (Edwards et al., 1987; Li et al., 1989), with recent developments in U-Pb dating offering the possibility of obtaining dates back to nearly 4 million yr (Woodhead et al., 2006). Meanwhile, their banded structure enables the environmental proxies recovered to be directly related to this chronological framework. Additionally, stalagmites provide stable post-depositional environments, with lipid biomarkers shown to be preserved for at least 100,000 yr (Rousseau et al., 1995). This offers the potential to recover firmly dated, detailed records of both climatically and anthropogenically driven vegetation change far back into pre-history, and beyond the limit of radiocarbon dating.

However, despite the long records available and the fact that biomarker signals in stalagmites have been shown to reflect changes in climate (Xie et al., 2003), until now it has not been possible to produce records with a temporal resolution better than several hundred years due to the large calcite samples required to obtain a clean and robust signal (Rousseau et al., 1995). This problem has recently been overcome by the development of an optimised sample preparation protocol (Blyth et al., 2006) and here we present the first high-resolution stalagmite biomarker record, using a sampling interval of 5 to 10 yr, and demonstrating how the plant-derived biomarkers preserved relate to changes in land use.

Site

The Mechara karst lies in south-eastern Ethiopia at the foot of a long mountain ridge marking the southeastern margin of the Ethiopian rift valley (Fig. 1). The cave systems are formed in the Jurassic Antalo Limestone (Bosellini et al., 1997; Asrat, 2002), which consists of massive crystalline limestones intercalated with marls and mudstone beds, changing to thin fossiliferous

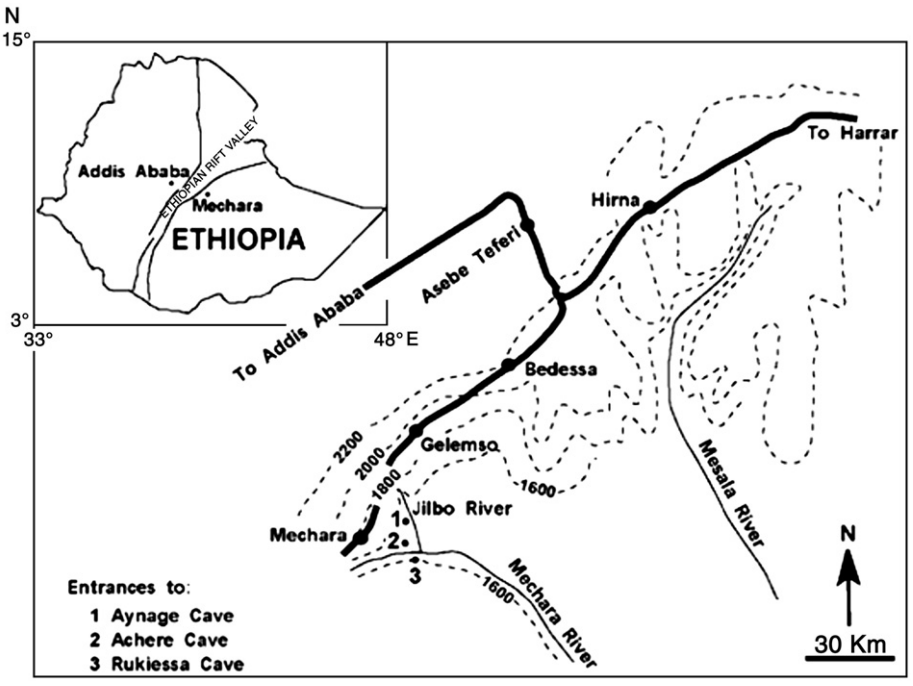

Figure 1. Map of Ethiopia showing location of Mechara karst.

limestones intercalated with sandy limestones and marls in the upper portion. The area is important in regional climate change studies, as it is very sensitive to the migration of the Inter-Tropical Convergence Zone, and to variations in the monsoons, resulting in strongly seasonal precipitation (which is reflected in the growth of the stalagmites), but a fairly constant temperature with an annual mean of 20–25 °C. Large numbers of fast-growing, clearly laminated stalagmites are found in the region, including specimens deposited over the past 10,000 yr suitable for long time-series analysis (Asrat et al., 2007), and actively growing stalagmites ideal for modern process work.

The sample reported here was collected from Asfa chamber in Rukiessa Cave (9°51.252′N, 37°65.1664′E). The cave is generally wet with cave streams and active drip-points and is subject to seasonal flash floods. Asfa chamber lies approximately 30 m beneath the surface and contains large numbers of active stalagmites. The roof of the cave is formed by a sandy limestone, above which thin (<1 m) residual soils have developed.

The surrounding area is currently agricultural, with the land above the cave dominated by ploughed fields producing a mixture of grains, chiefly tef (an ancient wild grain native to Ethiopia), maize (*Zea mays*) and millet (*Panicum miliaceum*)), and perennial cash crops (khat (*Catha edulis*) and coffee (*Caffea* sp.). Scattered patches of trees and scrub still exist around Rukiessa; these are the remnants of an earlier wooded vegetation regime, which was destroyed by one of the major agricultural clearances which occurred across many regions in Ethiopia during the 1930's (Machado et al., 1998).

Sample

Asfa-3, a small (40-mm-high) stalagmite, was collected from beneath an active drip point in Asfa Chamber, Rukiessa Cave, in 2004 (Baker et al., 2005). A young sample was specifically chosen for analysis, so that the biomarker signals obtained could be tested against the known history of local land use. Drip-water electrical conductivity was >700 μs cm^{-1} when sampled, indicating active deposition. Upon sectioning, the stalagmite was seen to be regularly laminated, with visible bands of white, brown and black calcite, the microscopic fabric of which was highly indicative of annual lamina deposition (see Baker et al., 2007). The sample is thus ideally suited to building an annual chronology with which to frame biomarker data. Laminae widths were therefore counted; growth rate has a well-understood relationship with surface climate, primarily driven by the production of soil CO_2 due to changes in temperature and moisture (Dreybrodt, 1981; Dreybrodt, 1988; Baker et al., 1998). To confirm modern growth, radiocarbon analyses were performed to determine the presence of 'bomb' ^{14}C.

Methods

Stalagmite growth rate is derived from visible lamina widths, which are determined by drip rate, changes in cave humidity and/or drip-water saturation (Genty and Quinif, 1996; Genty et al., 1997, 2001). Lamina counting was conducted on a scanned high-resolution image of the polished stalagmite using image processing software (Image Pro Plus 5.0) and the protocols outlined in Tan et al. (2006). The image was enhanced by stretching the observed range of pixel intensities to the maximum possible (full 0–255 range), and laminae widths calculated by measuring the average distance between visible laminae using a ~50 pixel wide transect. Triplicated lamina profiles were counted.

Stalagmites record the atmospheric ^{14}C input superimposed on the ^{14}C signal from 'dead carbon' that is derived from limestone dissolution (Genty and Massault, 1997, 1999; Genty et al., 1998, 2001). Stalagmite 'dead carbon proportion' is typically 15±10% in modern European stalagmites, and the superimposed 'atmospheric carbon' signal is both damped and has a time delay between the transfer of C from the atmosphere and its deposition in a stalagmite, due primarily to soil carbon cycling.

Speleothem samples were drilled and stored under argon until hydrolysis to CO_2 using 85% H_3PO_4 at 25 °C. Carbon dioxide was cryogenically purified. Aliquots of CO_2 were converted to an iron/graphite mix by iron/zinc reduction (Slota et al., 1987). A subsample of CO_2 was used to measure $\delta^{13}C$ using a dual-inlet mass spectrometer with a multiple ion beam collection facility (VG OPTIMA) in order to normalise ^{14}C data to −25‰ $\delta^{13}C_{VPDB}$. Graphite prepared at the NERC Radiocarbon Laboratory was analysed by Accelerator Mass Spectrometry at the Scottish Universities Environmental Research Centre AMS (5MV NEC) (Xu et al., 2004).

Oxygen and carbon isotopes in speleothem calcite provide records of one or both of rainfall source variations or temperature, together with a groundwater smoothing effect and potential kinetic fractionation effects (McDermott, 2004). Samples for stable isotope measurements were drilled at regular intervals along the central growth axis of Asfa-3. To avoid aliasing effects, time-integrated samples of 3–5 yr duration were drilled (1–3 mm depending on growth rate). In addition, samples were drilled laterally along growth laminae in order to investigate the lateral changes in isotope composition (the 'Hendy test'). Analyses were conducted at the NERC Isotope Geosciences Laboratory at Keyworth. The calcite samples were reacted with phosphoric acid and cryogenically purified before mass spectrometry using an Isocarb plus Optima dual inlet mass spectrometer. By comparison with a laboratory marble standard, the sample $^{18}O/^{16}O$ and $^{13}C/^{12}C$ ratios are reported as $\delta^{18}O$ and $\delta^{13}C$ values in per mil (‰) versus VPBD. Analytical precisions are <0.1‰ for the standard marble.

For lipid analysis, a central longitudinal slice of Asfa-3 was sectioned into 11 subsections (Fig. 2) with a temporal resolution of 5–10 yr (a calcite sample size of ca. 1 g). To remove surface contamination each subsample was ultrasonicated in 90:10 dichloromethane (DCM):methanol (5×3 min). The samples were digested in 3 M pre-cleaned hydrochloric acid and boiled under reflux for 2 h following Blyth et al. (2006). Internal standards Androstanol and 5β-Cholanic acid were added prior to reflux. Once cool, the lipids were extracted with DCM (30 ml×6) in a separating funnel and methylated using 3 ml of boron trifluoride–methanol complex (12% BF_3/methanol,

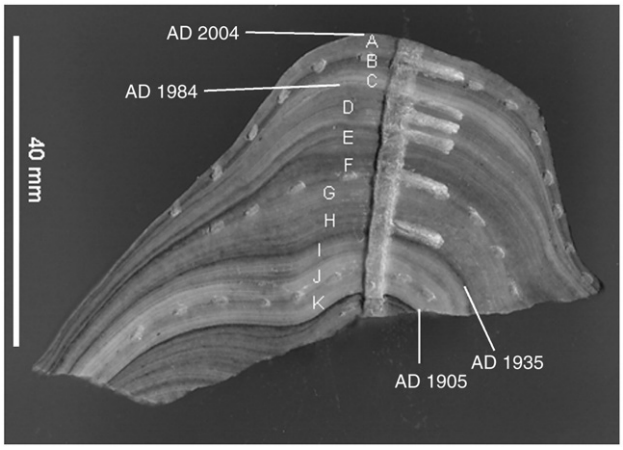

Figure 2. Asfa-3, showing sectioning scheme for lipid analysis.

Aldrich) for 2 h at 70 °C and overnight at room temperature. After destruction of the BF_3 complex with Milli-Q water (3 ml), and re-extraction with petroleum ether (2 ml × 6), the sample was further derivatised with 5 drops of BSTFA ($C_8H_{18}F_3NOSi_2$, Fluka Chemika) for 2 h at 70 °C, and left to stand at room temperature overnight.

Samples were analysed using a Hewlett Packard 6890 GC split/splitless injector (at 280 °C) linked to a Hewlett Packard 5973 MS detector, with the oven temperature ramped from 40 to 300 °C at 4 °C per min, and held at 300 °C for 20 min, carrier gas He, and ionisation energy of the MS set at 70 eV. The GC was equipped with an HP-1MS fused silica capillary column (30 m × 0.25 mm i.d.). Data acquisition was in selected ion mode. Lipid peaks were quantified on the appropriate ion chromatograms and calculated to μg/g calcite. They were also recalculated to a percentage of the total sum of measured lipids for each subsample, in order to remove stalagmite growth rate artefacts.

Results and discussion

Stalagmite age and growth rates

Lamina counts demonstrate the presence of 99 laminae through Asfa-3 from the top of the stalagmite to the base of band K. Errors on counting are ±4 laminae. Mean lamina width is 0.37 mm, which is in agreement with that predicted from Rukiessa Cave drip-waters (electrical conductivity of 678 ± 177 μS, calcium ion concentration of 44.3 ± 22.9 ppm). Cave air temperature is 22.0 ± 0.3 °C and CO_2 concentration ~1500 ppm: from these values, based upon the calculations proposed by Dreybrodt (1988), we can predict a modern stalagmite growth rate of ~0.2 to 0.3 mm yr^{-1}.

High electrical conductivities found in Asfa-3 are indicative of calcite saturation and are interpreted as indicators of active carbonate deposition. This interpretation is supported by the rising trend in percent modern carbon (%mc) towards the top of Asfa-3 (Table 1), with values exceeding 100%mc unequivocally indicating ^{14}C input from atmospheric nuclear weapons testing. This confirms that the topmost layers of Asfa-3 have been deposited since 1950 (Genty and Massault, 1997, 1999, Genty et al., 2001). Lamina years representing AD 1950 are equivalent to ^{14}C values (pMC) of ~90% for Asfa-3, indicating a 'dead carbon' percentage of approximately 10%, values that are typical for cave stalagmites (Vogel, 1983; Genty et al., 1998).

Lipid biomarker composition

High-molecular weight *n*-alkanes are present in the range of C_{25}–C_{33} and show a strong odd-over-even predominance, which is indicative of a vegetational origin. This can be measured by use of the Carbon Preference Index, or CPI (Bray and Evans, 1961), which provides a numerical representation of the dominance of odd or even chain lengths. The formula used here is the modified CPI2, formulated by Marzi et al. (1993):

$$\mathrm{CPI2} = 0.5 * \left[\frac{(C_{25}+C_{27}+C_{29}+C_{31})}{(C_{26}+C_{28}+C_{30}+C_{32})}\right] + \left[\frac{(C_{27}+C_{29}+C_{31}+C_{33})}{(C_{26}+C_{28}+C_{30}+C_{32})}\right]$$

This gives CPI = 1 if the *n*-alkanes are smoothly distributed, that is, if there is no chain-length predominance. Alkanes of a vegetational origin will therefore have a CPI of $\gg 1$.

Asfa-3 has an average CPI of 5.6, with a range from 2.8 at the base to 8.5 in the middle band of the sample. This indicates that the *n*-alkanes in the sample are predominantly derived from higher plant sources, but that the signal in the lower three bands, and in the top-most band which has a CPI of 3.3, contain a greater proportion of microbially derived material than the main bulk of the stalagmite.

Figure 3 shows the changing distribution of the C_{25}–C_{33} *n*-alkanes through time. At least two distinct phases can be seen, which correlate well with known changes in land use in the area.

In the first phase, recorded in laminae deposited between 1905 and 1935 (bands K-I), the distributions are dominated by C_{25} and C_{27} and are comparable to *n*-alkane distributions observed in woodland soils (Marseille et al., 1999). C_{27} is believed to be principally derived from the overlying trees, as it has frequently been found to be the dominant *n*-alkane in arboreal vegetation (Marseille et al., 1999), while increased quantities of C_{25} and C_{27} together have been attributed to fungal and microbial action within woodland and forest soil ecosystems (Marseille et al., 1999): the combined dominance of C_{25} and C_{27} in bands K-I of the stalagmite is thus consistent with the

Table 1
^{14}C results for Asfa-3, showing bomb carbon in the upper laminae

Publication code	Identifier	Lamina year	^{14}C enrichment (% modern ± 1σ)	Conventional radiocarbon age (yr BP ± 1σ)
SUERC-7016	Asfa-3A	2004	104.39 ± 0.31	post-1950
SUERC-8070	Asfa-3	1990	103.41 ± 0.31	post-1950
SUERC-8071	Asfa-3	1980	92.61 ± 0.28	616 ± 25
SUERC-8072	Asfa-3	1970	91.13 ± 0.28	746 ± 24
SUERC-8073	Asfa-3	1960	91.50 ± 0.28	713 ± 24
SUERC-8074	Asfa-3	1950	90.23 ± 0.27	826 ± 24

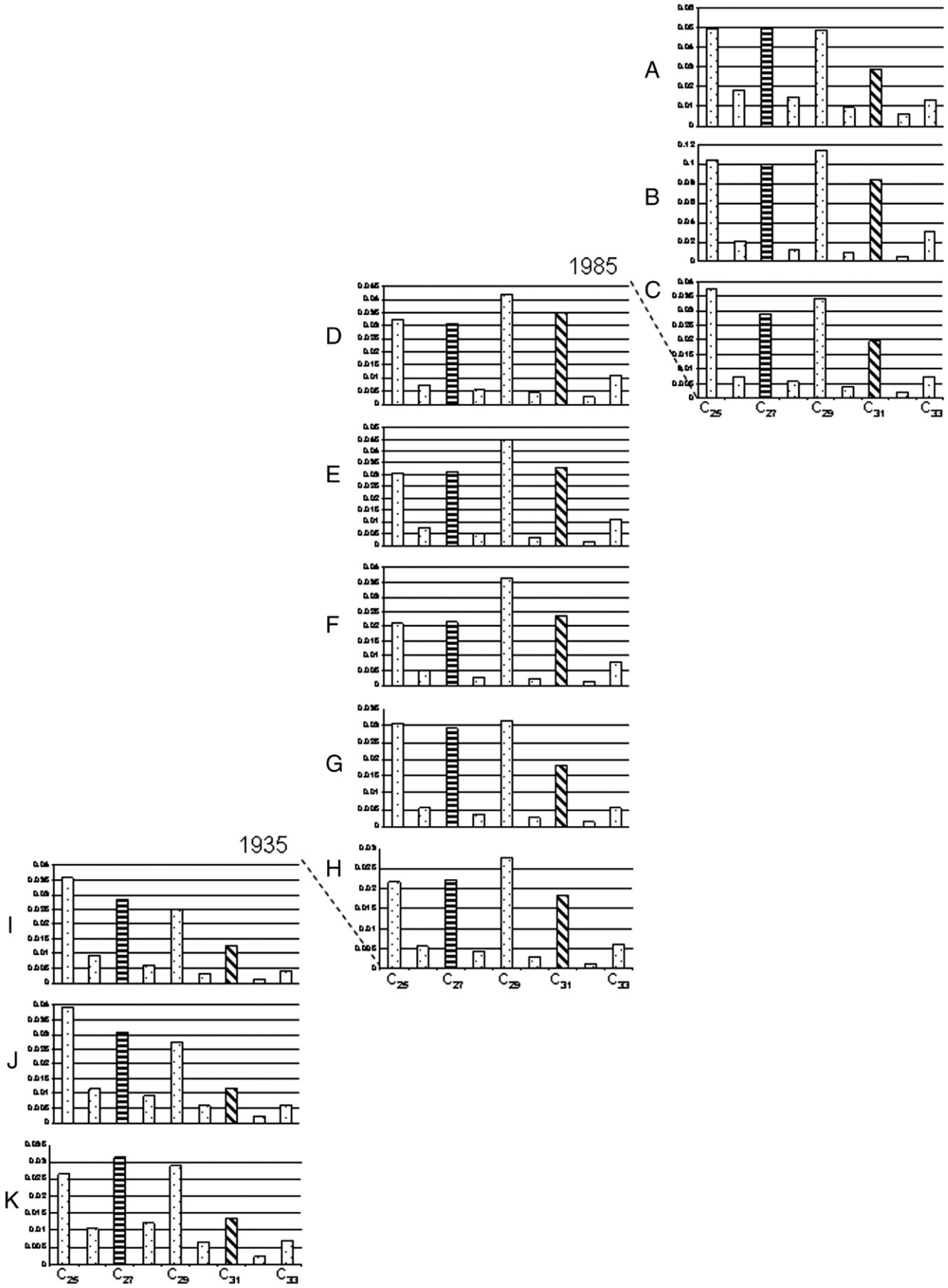

Figure 3. *n*-alkane distributions in Asfa-3 through time, showing differing amounts of C_{27} (horizontal shading) and C_{31} (diagonal shading).

lower CPI values of these bands. These distributions suggest an ecosystem dominated by scrub or woody vegetation with an underlying leaf litter subject to fungal and microbial degradation, and they are proposed as reflecting the original vegetation of the area that was cleared during the 1930's to make way for agriculture.

The second phase occurs from band H onwards (deposited from AD 1935 onwards) and represents a prolonged period of agricultural production in the surrounding area. This is seen in the *n*-alkanes as a relative decrease in C_{25} and C_{27}, and particularly by a substantial increase in C_{31}, which is apparent both in the *n*-alkane distributions and in the ratio of C_{27}/C_{31} (Fig. 4). This ratio is of particular interest as it has previously been proposed as a marker for arboreal vs. herbaceous plant input (Marseille et al., 1999). While C_{27} is one of the common dominant *n*-alkanes in trees, C_{31} is typically the dominant alkane in the leaf waxes of grasses and herbaceous vegetation (Rieley et al., 1991; Marseille et al., 1999) as well as both C3 and C4 crops (Wiesenberg et al., 2004), with soils cropped with maize showing notable C_{31} enrichment (Wiesenberg et al., 2004). The dominance of C_{29} in these distributions is proposed as resulting from either a high contribution of root-derived *n*-alkanes (Wiesenberg et al., 2004) or microbial action in the soil, with soil profiles under grass having previously been shown to move towards a C_{29}-dominated distribution with depth (Marseille et al., 1999). Figure 5 plots the relationship between the C_{27}/C_{31} *n*-alkane ratio and the CPI2: this clearly shows both the difference between bands K-I and the rest of the stalagmite (with the exception of band A, discussed below), and the relationship between the two parameters, with an increase in the CPI2 (representing fresh vegetation matter) being mirrored by a decrease in the *n*-alkane ratio (i.e., increased C_{31}).

The changes seen in the *n*-alkanes are mirrored in parameters relating to *n*-alkanols and *n*-fatty acids (Fig. 6), which compares the trends in the different lipid signals through time. Both the HMW *n*-alkanols and HMW *n*-fatty acids in Asfa-3 have a strongly even-over-odd carbon number predominance, indicating that they are chiefly derived from higher plants (Harwood and Russell, 1984; Jambu et al., 1993; Bull et al., 2000). Bands K-I are relatively depleted in the HMW *n*-acids and *n*-alcohols, while containing a relatively larger proportion of low molecular weight *n*-fatty acids (which are general across many parts of the ecosystem).

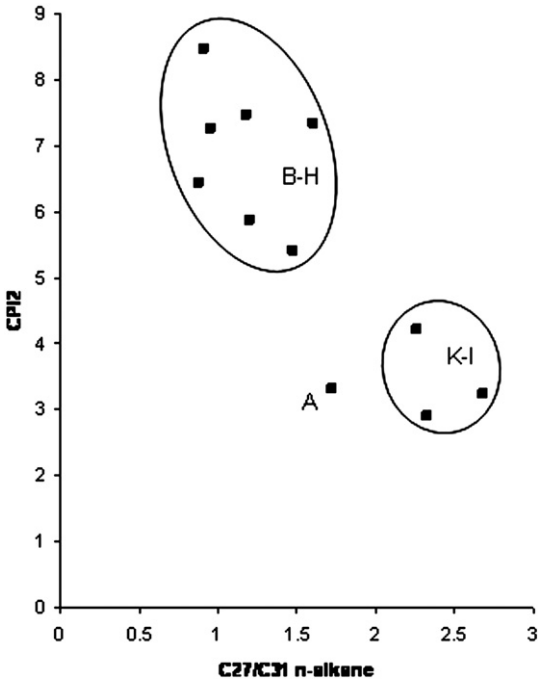

Figure 5. Plot of C_{27}/C_{31} *n*-alkane ratio against CPI2, showing the relationship between an increase in C_{31} *n*-alkanes and the input of fresh plant-derived material.

In detail, the increase in HMW *n*-alkanols is principally driven by increases in C_{26} and above. Most terrestrial plants, including most crop plants, have an *n*-alkanol dominance of C_{26} or C_{28}, but several trees have been shown to be more commonly dominated by C_{24} (Bull et al., 2000). Therefore, enrichment in the longer chain lengths would be expected with a change from woodland to agriculture. The changes in the ratio of C_{24}/C_{28} *n*-alkanol through Asfa-3 closely mirror those seen in the C_{27}/C_{31} *n*-alkane ratio (Fig. 6), with C_{24} dominating in bands K-I followed by a change in favour of C_{28} through the middle of the 20th century.

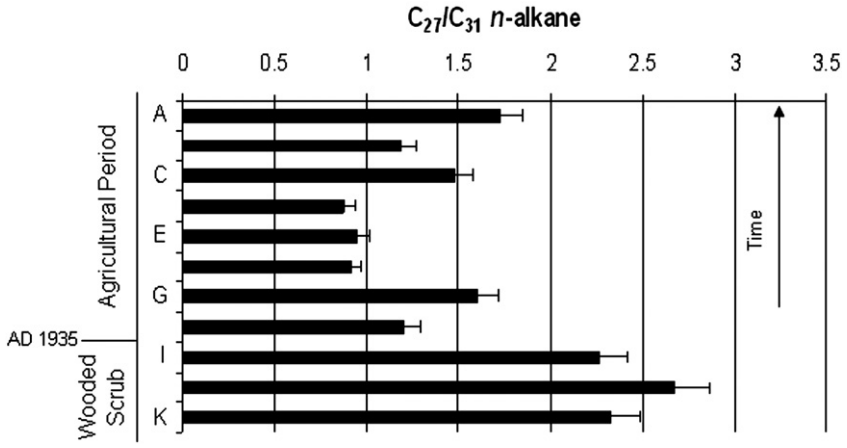

Figure 4. C_{27}/C_{31} *n*-alkane ratio through time. Note the decrease in favour of C_{31} at AD 1935. Error bars are for methodological replicates and are 1 SD ($n=5$).

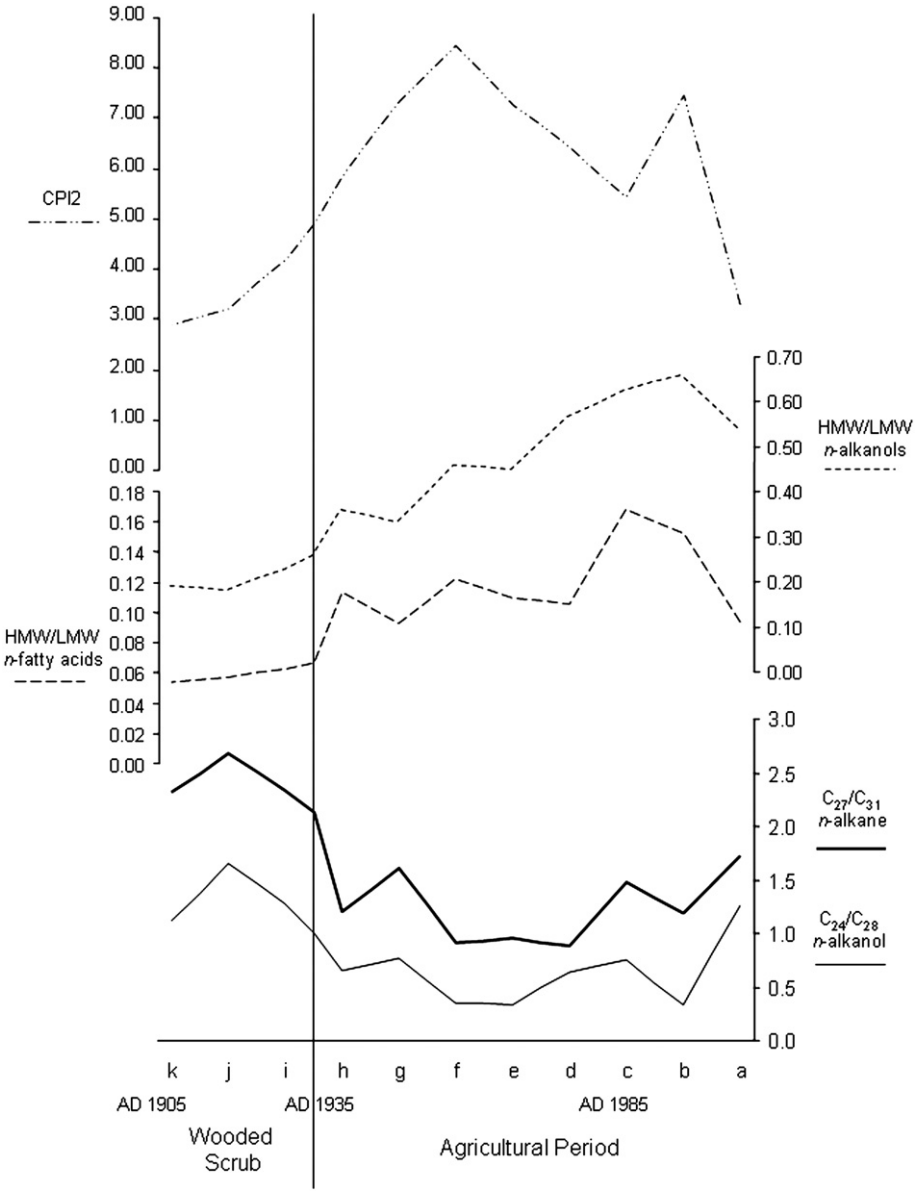

Figure 6. Comparison of the different lipid trends through time in Asfa-3. From the top of figure: CPI2; ratio of HMW/LMW *n*-alkanols; ratio of HMW/LMW *n*-fatty acids; ratio of C_{27}/C_{31} *n*-alkane; ratio of C_{24}/C_{28} *n*-alkanol.

The changes in the acids are more complex to interpret as they could relate to either changes in vegetation type, which has been shown among crops to affect the chain length distribution of *n*-fatty acids in soils (Wiesenberg et al., 2004), or to changes in the soil environment (Amblès et al., 1989; van Bergen et al., 1998). The presence of degraded plant matter in the soil has been proposed as a major mechanism for enriching HMW *n*-fatty acid levels (Wiesenberg et al., 2004), and this would be expected to occur with agricultural regimes where residual plant material is ploughed back into the soil after crop harvesting.

There are changes in the lipid signal at other points in the time series, but none of these are as marked as that at the top of band I, and they do not show the same degree of simultaneous variation across several parameters. The most notable of these other changes is in band A, which has weak similarities to bands K-I in several of the parameters and substantial correlation in the CPI2 (Fig. 5). We propose that there may be a third agricultural phase apparent here, reflecting an increase in the production of perennial cash crops, and particularly khat. A trend for the intercropping of khat and cereals has become dominant across much of the southeastern Ethiopian Highlands in recent years, as khat offers higher export returns and increased drought resistance compared to either cereals or other cash crops (Mulatu and Kassa, 2001; Feyisa and Aune, 2003). No detailed studies of the biomarker compositions in the soil beneath khat cropped areas are available; however, it is a tree-like shrub and is often inter-planted with coffee, both of which are, in turn, planted under the shade of larger trees, so a return towards the lipid composition associated with wooded ground would not be surprising.

Comparison with stable isotope profiles

The detailed interpretation of the ^{18}O time series (Fig. 7) is reported in Baker et al. (2007). By correlating ^{18}O against monthly rainfall data, a complex correlation with surface climate was demonstrated, with the time series correlating with both the isotopic composition of spring and summer rains and with fractionation processes due to non-equilibrium calcite formation during continued dripping from the storage-flow component in the winter dry season. Correlations with climate were stronger at a decadal average, demonstrating the importance of a storage-flow component.

Despite this stored component, however, the $\delta^{13}C$ profile shows high-resolution structure. The most significant event is at ~AD 1952, where the signal passes a threshold to lower values (a change of over 2‰). The Hendy tests reported in Baker et al. (2007) demonstrate that although some kinetic fractionation effects are apparent, they are routinely under 1‰ and so not sufficient for this change to be attributed to fractionation alone. Therefore, an environmental control on the isotopic signal is also indicated. Substantial changes in stalagmite $\delta^{13}C$ values have often been proposed as relating to changes in the overlying vegetation type (e.g., Dorale et al., 1998), as plants using different photosynthetic pathways release a different isotopic signal into the soil (Cerling, 1984). It seems unlikely that the isotopic change in Asfa-3 is a direct reflection of vegetation type, as the fluctuation is relatively small in this context and the signal is moving in the opposite direction to that which might be expected with an increase in agriculture. The reported agricultural history of the area indicates that the principal crops planted at this time were tef, maize and millet, which are all C4 plants: therefore, if vegetation type was driving the isotopic change, we would expect it to manifest as increase in the $\delta^{13}C$ values, since C4 plants are more enriched in ^{13}C than C3 vegetation (Cerling, 1984).

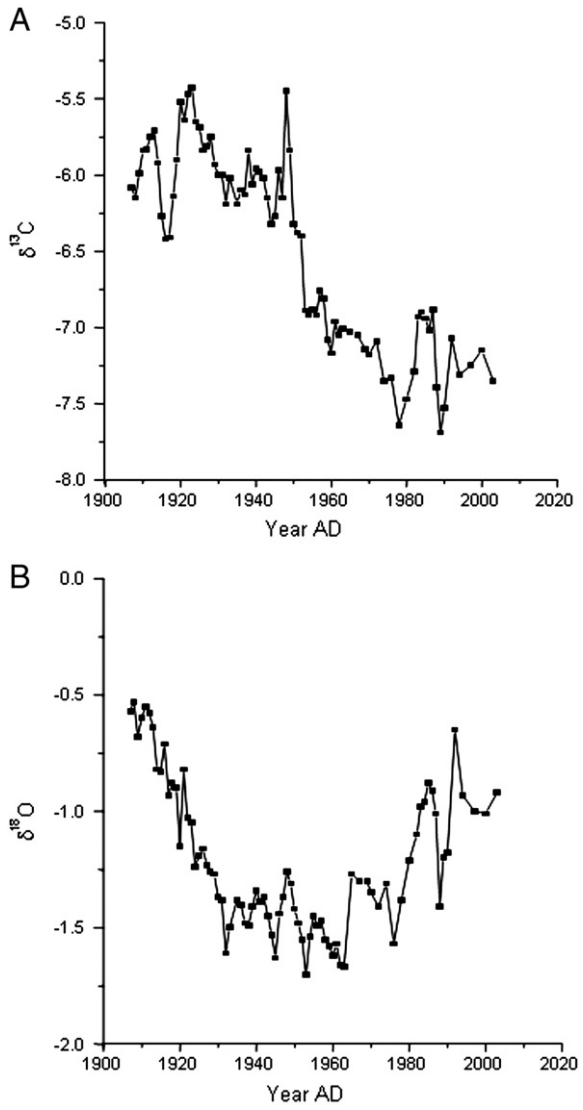

Figure 7. (A) $\delta^{13}C$ through Asfa-3, (B) $\delta^{18}O$ through Asfa-3.

To resolve this issue for certain would require examination of the compound-specific carbon isotopic signal of the plant-derived molecules preserved in stalagmites from the region. However, we propose that another mechanism is driving the stable carbon isotope signal. Depleted $\delta^{13}C$ values have previously been interpreted as a response to increases in vegetational development and plant cover, causing a greater input of isotopically light biogenic carbon (Genty et al., 2003, 2006; Baldini et al., 2005). Although this initially seems contradictory to the known history of deforestation in the area, we suggest that the change in the $\delta^{13}C$ is triggered by a similar mechanism resulting from an increase not in plant *cover*, but in plant material *input* to the soil resulting from agricultural practices. This is supported by the lipid signal, which shows that agricultural development in the area was accompanied by an increase in vegetational biomarkers such as HMW *n*-fatty acids and *n*-alkanols, as well as an increase in the CPI2, all of which suggest that the amount of plant matter entering the system has been increased.

Temporal lags

One important issue when considering environmental proxies preserved in stalagmites is that of temporal lags: the delay between a chemical signal being created in the surface environment and its preservation in the cave. The length of this delay is controlled by the rate of production, the turnover of organic matter within the soil and the hydrogeological pathways sourcing the drip which feeds the stalagmite. Tracer studies have shown that water fed through fissures in the rock moves more quickly than that permeating through pores (Einsiedl, 2005). The type of rock and depth of the cave chamber will also have an impact (Baker et al., 1996). The result of a long temporal lag will be a smoothing of environmental signals, as waters mix in the aquifer. In the case of lipid biomarkers, there is also potential for a reduction or even destruction of part of the signal, as lipids can degrade over time with oxidation or bacterial reworking in either the aquifer or the soil (van Bergen et al., 1998; Bull et al., 2000). This issue has not previously been addressed in studies of lipids in stalagmites, as the

temporal resolution involved in studies such as Xie et al. (2003) has been too broad to be affected. However, with storage lags in pore-fed water at one site having been recorded at an average of 62 yr (Einsiedl, 2005), this is obviously an important issue in the recovery of the high-resolution signals required to detect sudden events such as land-use change.

To identify delays resulting from soil carbon turnover, we can use the ^{14}C analyses of the stalagmite and utilise the ^{14}C modelling of Genty et al. (1998; 2001). The model fit to our stalagmite ^{14}C data is shown in Figure 8 and highlights the necessity of having a soil carbon pool of intermediate age (90 yr) as the predominant (80%) carbon pool (for discussion of the assumptions underlying the model, see Genty et al., 1998). This effect is clearly seen in the actual lag between the bomb ^{14}C peak in the atmospheric and stalagmite signals, the latter of which shows a delayed response to the atmospheric bomb spike and an attenuated or damped signal. This relatively smooth ^{14}C profile with a long lag to a very damped bomb ^{14}C peak is typical of that observed in stalagmites with thick soil cover and a large, slow-turnover soil carbon reservoir (Genty and Baker, in press).

A similar situation is seen in two hydrological pathways hypothesised to be feeding the stalagmite: rapid flow 'event' water transported within a year and storage water with decadal-scale turnover. If Asfa-3 is completely dominated by the storage-flow component, then highly smoothed $\delta^{18}O$ and $\delta^{13}C$ profiles would be expected, while if the fast-flow pathway dominates, we would expect to see response to known high-resolution climatic events. The stable isotope profiles do show some structure at an annual resolution (Fig. 7), especially the change in $\delta^{13}C$ at ~AD 1952, but in general there is only a weak relationship with recorded climate and environmental change.

The lipid signals preserved in the stalagmite do not show a smoothed or significantly lagged signal based upon laminae counting, however; instead, there are clear and abrupt changes occurring in both the chain length distribution and the C_{27}/C_{31} ratio of the *n*-alkanes, as well as changes in the proportional abundances of the *n*-fatty acids and the *n*-alkanols. These all show a close and coherent correspondence to the known vegetational history of the surrounding area, and they indicate a near-immediate response of the stalagmite lipids to changes in the overlying environment. This suggests that the active biomarker signal seen is predominantly being drawn from the fast-turnover carbon pool and transported via the rapid-flow pathway. The precise mechanism for this is currently subject to further investigation, but our preferred hypothesis is that the lipids in the slow carbon reservoir and the stored water have degraded over time, leaving compounds transported via the fast pathways to dominate over any underlying smoothed lipid signal.

Conclusion

Changes in the distribution of HMW *n*-alkanes and *n*-alkanols preserved in stalagmites have been shown to have the potential to record changes in vegetation regime and land use at a resolution of ~10 yr. Significantly, this signal does not seem to be affected by substantial temporal lags, allowing it to record events that are not apparent in other proxies such as stable carbon isotopes. Further work is now underway to test the repeatability of the signal across different stalagmites from the area and in different regions that have experienced significant vegetation changes at known periods in time. Combined with work to recover more vegetation-specific biomarkers and compound-specific carbon isotopes, this should provide a

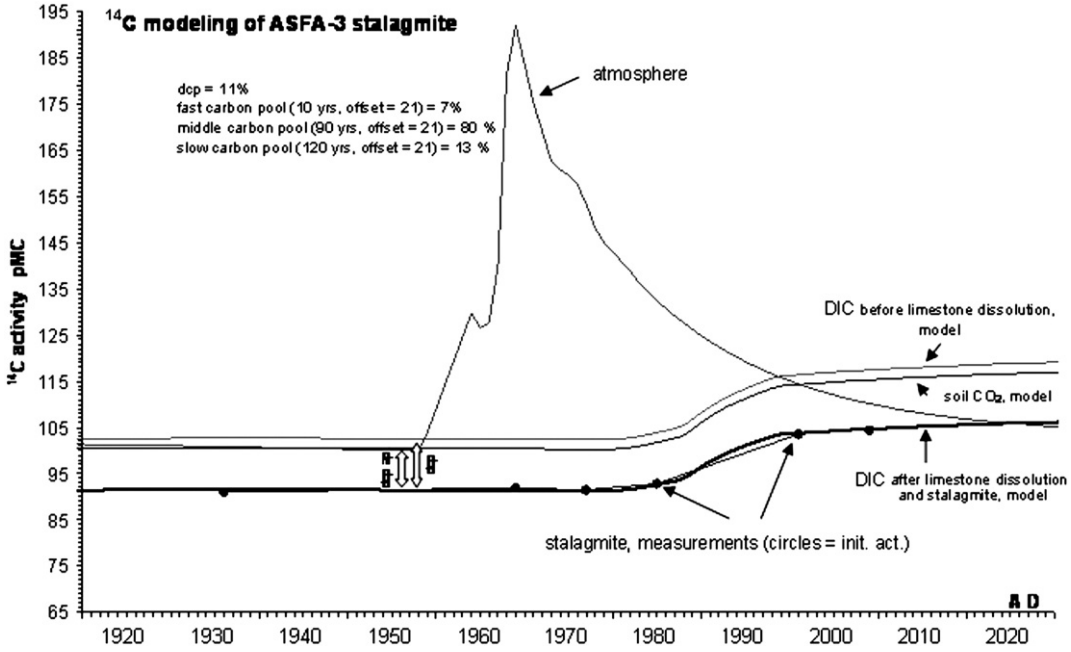

Figure 8. Model for atmospheric and dead carbon in Asfa-3. The extension of the graph past the present day is the modelled future stalagmite ^{14}C based on a continuing rate of decline of atmospheric ^{14}C and constant model soil carbon turnover conditions.

robust supporting data set, allowing the technique to be applied with confidence to palaeoenvironmental and archaeological records.

Acknowledgments

This work was supported by NERC studentship NER/S/A/2003/11297 awarded to Blyth, a Royal Society International Exchange Grant to Asrat and Baker, a Phillip Leverhulme Prize to Baker, a START-PACOM Grant to Asrat and NERC Radiocarbon support (1096.1004) to Baker and Ian Fairchild (University of Birmingham). Special thanks are offered to Sheik Mohammed Ahmed Surre, Imam of the Grand Mosque, Mechara, who provided in-depth information on the agricultural history of the area. Paul Donohoe provided invaluable assistance and support for GC-MS analysis, Paul Hands provided rock preparation facilities, Peter Wynn drilled the ^{14}C samples and Hilary Sloane undertook the stable isotope analyses. We also thank Peter Smart, Paul Farrimond, Jay Quade and two anonymous reviewers for their comments on the manuscript.

References

Amblès, A., Magnoux, P., Jambu, P., Jacquesy, R., Fustec, E., 1989. Effects of addition of bentonite on the hydrocarbon fraction of a podzol (A_1 Horizon). Journal of Soil Science 40, 685–694.

Asrat, A., 2002. Hewn churches of Central and Eastern Tigrai: A geological perspective. Geoarchaeology 17, 649–663.

Asrat, A., Baker, A., Umer, M., Leng, M.J., van Calsteren, P., Smith, C., 2007. A high-resolution multi-proxy stalagmite record from Mechara, Southeastern Ethiopia: Palaeohydrological implications for speleothem palaeoclimate reconstruction. Journal of Quaternary Science 22, 53–63.

Baker, A., Barnes, W.L., Smart, P.L., 1996. Speleothem luminescence intensity and spectral characteristics: Signal calibration and a record of palaeovegetation change. Chemical Geology 130, 65–76.

Baker, A., Genty, D., Dreybrodt, W., Grapes, J., Mockler, N.J., 1998. Testing theoretically predicted stalagmite growth rate with recent annually laminated stalagmites: Implications for past stalagmite deposition. Geochimica Cosmochimica Acta 62, 393–404.

Baker, A., Asrat, A., Umer, M., 2005. Expedition report to the Mechara caves, South-eastern Ethiopia. Speleology 18–20.

Baker, A., Asrat, A., Fairchild, I., Leng, M.J., Wynn, P., Genty, D., Umer, M., Bryant, C., 2007. Annual resolution climate reconstruction in Ethiopia using multiple stalagmite parameters: Modern climate calibration. Geochimica et Cosmochimica Acta 71, 2975–2988.

Baldini, J.U.L., McDermott, F., Baker, A., Baldini, L.M., Mattey, D.P., Railsback, L.B., 2005. Biomass effects on stalagmite growth and isotope ratios: A 20th century analogue from Wiltshire, England. Earth and Planetary Science Letters 240, 486–494.

Blyth, A.J., Farrimond, P., Jones, D.M., 2006. An optimised method for the extraction and analysis of lipid biomarkers from stalagmites. Organic Geochemistry 37, 882–890.

Bosellini, A., Russo, A., Fantozzi, P.L., Assefa, G., Tadesse, S., 1997. The Mesozoic succession of the Mekele Outlier (Tigrai Province Ethiopia). Memorie di Scienze Geologiche 49, 95–116.

Brassell, S.C., Eglinton, G., Marlowe, I.T., Pflaumann, U., Sarnthein, M., 1986. Molecular stratigraphy: A new tool for climatic assessment. Nature 320, 129–133.

Bray, E.E., Evans, E.D., 1961. Distribution of *n*-paraffins as a clue to recognition of source beds. Geochimica Cosmochimica Acta 22, 2–15.

Bull, I.D., van Bergen, P.F., Nott, C.J., Poulton, P.R., Evershed, R.P., 2000. Organic geochemical studies of soils from the Rothamsted classical experiments—V. The fate of lipids in different long-term experiments. Organic Geochemistry 31, 389–408.

Cerling, T.E., 1984. The stable isotopic composition of modern soil carbonate and its relationship to climate. Earth and Planetary Science Letters 71, 229–240.

Dark, P., 2006. Climate deterioration and land-use change in the first millennium BC: Perspectives from the British palynological record. Journal of Archaeological Science 33, 1381–1395.

Dimbleby, G., 1985. The Palynology of Archaeological Sites. Academic Press, London.

Dorale, J.A., Edwards, R.L., Ito, E., González, L.A., 1998. Climate and vegetation history of the Midcontinent from 75 to 25 ka: A speleothem record from Crevice Cave, Missouri, USA. Science 282, 1871–1874.

Dreybrodt, W., 1981. The kinetics of calcite deposition from thin films of natural calcareous solutions and the growth of speleothems: Revisited. Chemical Geology 32, 237–245.

Dreybrodt, W., 1988. Processes in Karst Systems. Wiley, New York.

Edwards, R.L., Chen, J.H., Wasserburg, G.J., 1987. ^{238}U–^{234}U–^{232}Th–^{230}Th systematics and the precise measurement of time over the last 500,000 years. Earth and Planetary Science Letters 81, 175–192.

Eglinton, G., Hamilton, R.J., 1967. Leaf epicuticular waxes. Science 156, 1322–1334.

Einsiedl, F., 2005. Flow system dynamics and water storage of a fissured-porous karst aquifer characterised by artificial and environmental tracers. Journal of Hydrology 312, 312–321.

Feyisa, T.H., Aune, J.B., 2003. Khat expansion in the Ethiopian Highlands–effects on the farming system in Habro District. Mountain Research and Development 23 (2), 185–189.

Genty, D., Baker, A., in press. Radiocarbon in speleothems. In: Burns, S. (ed) Speleothems and paleoclimate. Blackwell, Oxford.

Genty, D., Massault, M., 1997. Bomb ^{14}C recorded in laminated speleothems—Part 1: Dead carbon proportion calculation. Radiocarbon 39, 33–48.

Genty, D., Massault, M., 1999. Carbon transfer dynamics from bomb-^{14}C and $d^{13}C$ time series of a laminated stalagmite from SW France-Modelling and comparison with other stalagmite records. Geochimica et Cosmochimica Acta 63, 1537–1548.

Genty, D., Quinif, Y., 1996. Annually laminated sequences in the internal structure of some Belgian stalagmites—importance for paleoclimatology. Journal of Sedimentary Research 66, 275–288.

Genty, D., Baker, A., Barnes, W.L., 1997. Comparaison entre les lamines luminescentes et les lamines visibles annuelles de stalagmites. Comptes Rendus Acad. Sci. II 325, 193–200.

Genty, D., Vokal, B., Obelic, B., Massault, M., 1998. Bomb ^{14}C Time History Recorded in two modern stalagmites-Importance for soil organic matter dynamics and bomb ^{14}C distribution over continents. Earth and Planetary Science Letters 160, 795–809.

Genty, D., Baker, A., Vokal, B., 2001. Inter and intra annual growth rates of European stalagmites. Chemical Geology 176, 193–214.

Genty, D., Blamart, D., Ouahdi, R., Gilmour, M., Baker, A., Jouzel, J., Van-Exter, S., 2003. Precise dating of Dansgaard–Oeschger climate oscillations in western Europe from stalagmite data. Nature 421, 833–837.

Genty, D., Blamart, D., Ghaleb, B., Plagnes, V., Causse, Ch., Bakalowicz, M., Zouari, K., Chkir, N., Hellstrom, J., Wainer, K., Bourges, F., 2006. Timing and dynamics of the last deglaciation from European and North African $\delta^{13}C$ stalagmite profiles–comparison with Chinese and South Hemisphere stalagmites. Quaternary Science Reviews 25, 2118–2142.

Harwood, J.L., Russell, N.J., 1984. Lipids in Plants and Microbes. George Allen and Unwin, London.

Horrocks, M., Lawlor, I., 2006. Plant microfossil analysis of soils from Polynesian stonefields in South Auckland, New Zealand. Journal of Archaeological Science 33, 200–217.

Huang, Y., Street-Perrott, F.A., Perrott, R.A., Metzger, P., Eglinton, G., 1999. Glacial–interglacial environmental changes inferred from molecular and compound specific $\delta^{13}C$ analyses of sediments from Sacred Lake, Mt. Kenya. Geochimica et Cosmochimica Acta 63 (9), 1383–1404.

Jambu, P., Amblès, A., Jaquesy, J.C., Secouet, B., Parlanti, E., 1993. Incorporation of natural alcohols from plant residues into a hydromorphic forest-podzol. Journal of Soil Science 44, 135–146.

Lauritzen, S.-E., Lundberg, J., 1999. Speleothems and climate: A special issue of The Holocene. The Holocene 9, 643–647.

Li, W.X., Lundberg, J., Dickin, A.P., Ford, D.C., Schwarcz, H.P., McNutt, R., Williams, D., 1989. High-precision mass spectrometric uranium—Series dating of cave deposits and implications for palaeoclimatic studies. Nature 339, 534–536.

Machado, M.J., Pérez-González, A., Benito, G., 1998. Paleoenvironmental changes during the last 4000 yrs in the Tigray, Northern Ethiopia. Quaternary Research 49, 312–321.

Marseille, F., Disnar, J.R., Guillet, B., Noack, Y., 1999. *n*-Alkanes and free fatty acids in humus and A1 horizons of soils under beech, spruce and grass in the Massif-Central (Mont-Lozère), France. European Journal of Soil Science 50, 433–441.

Marzi, R., Torkelson, B.E., Olson, R.K., 1993. A revised carbon preference index. Organic Geochemistry 20, 1303–1306.

McDermott, F., 2004. Palaeo-climate reconstruction from stable isotope variations in speleothems: A review. Quaternary Science Reviews 23, 901–918.

Meyers, P.A., 1997. Organic geochemical proxies of palaeoceanographic, palaeolimnologic, and palaeoclimatic processes. Organic Geochemistry 27, 213–250.

Mulatu, E., Kassa, H., 2001. Evolution of smallholder mixed farming systems in the Harar Highlands of Ethiopia: The shift towards trees and shrubs. Journal of Sustainable Agriculture 18 (4), 81–112.

Nott, C.J., Xie, S., Avsejs, L.A., Maddy, D., Chambers, F.M., Evershed, R.P., 2000. *n*-Alkane distributions in ombrotrophic mires as indicators of vegetation change related to climatic variation. Organic Geochemistry 31, 231–235.

Pancost, R.D., Bass, M., van Geel, B., Sinninghe-Damsté, J.S., 2002. Biomarkers as proxies for plant inputs to peats: An example from a subboreal ombrotrophic bog. Organic Geochemistry 33, 675–690.

Rieley, G., Collier, R.J., Jones, D.M., Eglinton, G., 1991. The biogeochemistry of Ellesmere Lake, U.K.–I: Source correlation of leaf wax inputs to the sedimentary lipid record. Organic Geochemistry 17, 901–912.

Rousseau, L., Laafar, S., Pèpe, C., De Lumley, H., 1995. Sterols as biogeochemical markers: Results from Ensemble E of the stalagmitic floor, Grotte Du Lazaret, Nice, France. Quaternary Science Reviews 14, 51–59.

Slota, P.J., Jull, A.J.T., Linick, T.W., Toolin, L.J., 1987. Preparation of small samples for ^{14}C accelerator targets by catalytic reduction of CO_2. Radiocarbon 29, 303–306.

Tan, M., Baker, A., Genty, D., Esper, J., Cai, B., 2006. Applications of stalagmite laminae to palaeoclimate reconstructions: Comparison with dendrochronology/climatology. Quaternary Science Reviews 25, 2103–2117.

van Bergen, P.F., Nott, C.J., Bull, I.D., Poulton, P.R., Evershed, R.P., 1998. Organic geochemical studies of soils from the Rothamsted Classical Experiments—IV. Preliminary results from a study of the effect of soil pH on organic matter decay. Organic Geochemistry 29, 1779–1795.

Vogel, J.C., 1983. ^{14}C variations during the Upper Pleistocene. Radiocarbon 25, 213–218.

Wiesenberg, G.L.B., Schwarzbauer, J., Schmidt, M.W.I., Schwark, L., 2004. Source and turnover of organic matter in agricultural soils derived from *n*-alkane/*n*-carboxylic acid compositions and C-isotope signatures. Organic Geochemistry 35, 1371–1393.

Woodhead, J., Hellstrom, J., Maas, R., Drysdale, R., Zanchetta, G., Devine, P., Taylor, E., 2006. U-Pb geochronology of speleothems by MC-ICPMS. Quaternary Geochronology 1, 208–221.

Xie, S., Yi, Y., Huang, J., Hu, C., Cai, Y., Collins, M., Baker, A., 2003. Lipid distribution in a subtropical southern China stalagmite as a record of soil ecosystem response to palaeoclimate change. Quaternary Research 60, 340–347.

Xu, S., Anderson, R., Bryant, C., Cook, G.T., Dougans, A., Freeman, S., Naysmith, P., Schnabel, C., Scott, E.M., 2004. Capabilities of the new SUERC 5MV AMS facility for ^{14}C dating. Radiocarbon 46, 59–64.